

# Design, development and evaluation of an 8 $\mu$ PPT propulsion module for a 3U CubeSat application

IEPC-2011-115

*Presented at the 32<sup>nd</sup> International Electric Propulsion Conference,  
Wiesbaden, Germany  
September 11–15, 2011*

Shaw P. V. \* Lappas V. J. †  
and Underwood C. I. ‡

*University of Surrey, Guildford, Surrey, GU2 7XH, UK*

CubeSats to date have shown an excellent potential in providing quality science and demonstrating the use of COTS technology in space applications. A next stage in the evolution of CubeSat technology is the ability to demonstrate useable on board propulsion. A propulsion flight module has been designed and developed that will be able to provide pitch, roll and yaw around a central axis and translational movement in two axes. The module comprises of eight parallel bar micro Pulsed Plasma Thrusters ( $\mu$ PPTs). To aid in the miniaturisation there have been two significant changes. The first was a replacement of the typical sparkplug with a contact trigger mechanism that initiates a discharge. The second was the removal of the typical Teflon<sup>TM</sup> propellant bar used in PPTs between the discharging electrodes. In studies at the Surrey Space Centre it was shown that discharges without the presence of Teflon<sup>TM</sup> produced  $\approx$  60-75% the impulsebit (based on integral calculations of the averaged current discharge profiles) compared to discharges which had the presence of Teflon<sup>TM</sup> between the electrodes, at the parameters that were tested. The mass eroded for the plasma production was theorised to originate from the electrodes, which is similar in the mechanisms of operation to the Vacuum Arc Thruster (VAT). The module is split into three PC104 boards, two boards house four  $\mu$ PPTs and the third board is the power unit. The power unit uses award winning miniature voltage multipliers that take the 5V CubeSat bus voltage and transforms this to 800V for the PPT high voltage capacitors. This paper focuses on the developmental work that has been conducted to construct a propulsion module for the Surrey Training Research and Nano-satellite Demonstration (STRaND) 3U CubeSat.

## Nomenclature

$I_{bit}$	= Impulse bit, N.s
$L'$	= Inductance per unit length, $\text{Hm}^{-1}$
$I$	= Current, A
$\mu_0$	= Permeability of free space, $\text{NA}^{-2}$
$h$	= Separation distance between electrodes, m
$w$	= Width of electrodes, m

---

\*Research Assistant, Surrey Space Centre, p.shaw@surrey.ac.uk

†Reader, Surrey Space Centre, v.lappas@surrey.ac.uk

‡Deputy Director, Surrey Space Centre, c.underwood@surrey.ac.uk

## I. Introduction

The CubeSat is a disruptive technology; with its low production cost and ever-increasing payload capability this technology has the possibility of seriously impacting the economics of space. Surrey Satellite Technology Limited (SSTL) will be developing and exploiting CubeSats as a relatively cost effective approach to provide training and demonstration of new technologies on a 3U CubeSat platform. The Surrey Technology Research and Nanosatellite Demonstration mission (STRaND-1) will be a precursor technology demonstration mission for a series of follow on missions. To increase the satellites in-orbit lifetime a propulsion system will need to be developed to compensate for drag and in-orbit manoeuvring. The SSTL inhouse  $\mu$ resistor jet with propellant tank and feedlines proved to be too cumbersome for a full axis control system. In collaboration with the Surrey Space Centre (SSC) an alternative propulsion module was proposed that utilised one resistojet thruster and a system of eight  $\mu$ PPTs. This was accepted as part of the ADCS system.

## II. $\mu$ PPT Design Phase

Previous experimental work showed that a standard breech fed parallel plate PPT could sufficiently operate with and without a Teflon<sup>TM</sup> propellant bar being present.<sup>1</sup> The impulse bit  $I_{bit}$  of the discharge can be estimated using the following relationship;

$$I_{bit} = L' \int I^2 dt = \frac{1}{2} \mu_0 \frac{h}{w} \int I^2 dt \quad (1)$$

It has been reported that Equation 1 has a tendency to over predict the impulse bit. A number of empirical alternatives have been reported for the inductance per unit length,  $L'$ .<sup>2</sup> However in all cases the inductance per unit length is thought to be a constant and the time varying significant factor is the current. Although the specific value of the impulse bit in the following plots may be inaccurate the trends that are seen are still significant, see Figure 1. The plot shows that the performance of the PPT without Teflon<sup>TM</sup> was approximately 60-75% of the performance with Teflon<sup>TM</sup>.

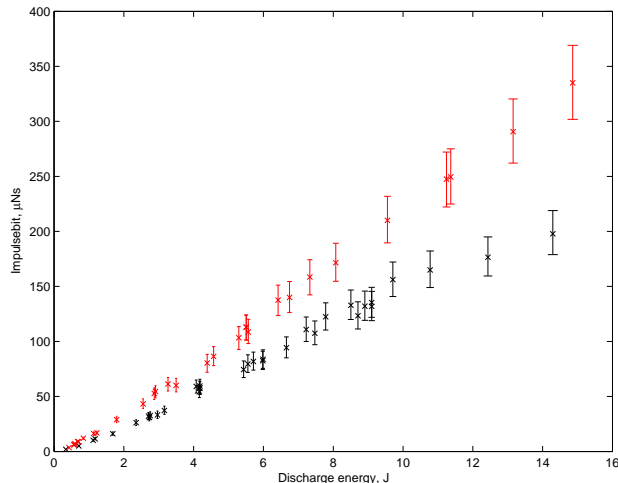


Figure 1. Combined data sets showing how the impulse bit relates to the PPT discharge energy when Teflon<sup>TM</sup> is present (red) and is not present (black) between the electrodes

The decision to remove Teflon<sup>TM</sup> from the PPT was taken for two reasons. The first was that by removing the Teflon<sup>TM</sup> bar and the feed mechanism, valuable space and volume would be saved. Secondly, Teflon<sup>TM</sup> contains chains of carbon, which when broken down, would coat the inside surface of the thruster with a film of carbon. When enough carbon builds up on the surfaces connecting the two electrodes it would lead to arc tracking and failure of the PPT, removing the source of the carbon could lead to an extension in the lifetime of the thruster.

The iterative design process began by modelling a PPT with similar characteristics to the one tested experimentally, results shown in Figure 1, so a capacitance of  $4\mu\text{F}$  was chosen for the capacitor. The voltage rating of the capacitor dictated its size, the higher the voltage rating the larger the capacitor would be. An

initial voltage rating of 700V was chosen for the CubeSat PPT as this was the minimum voltage during experimentation at which the PPT would regularly discharge.

The electrode spacing and geometry was chosen based on the knowledge gained from testing that showed an optimum in spacing between the electrodes to be between 10mm to 30mm, see Figure 2. The electrode separation was chosen to be within this range but was limited to 11mm to allow for the placement of four PPTs into a single module.

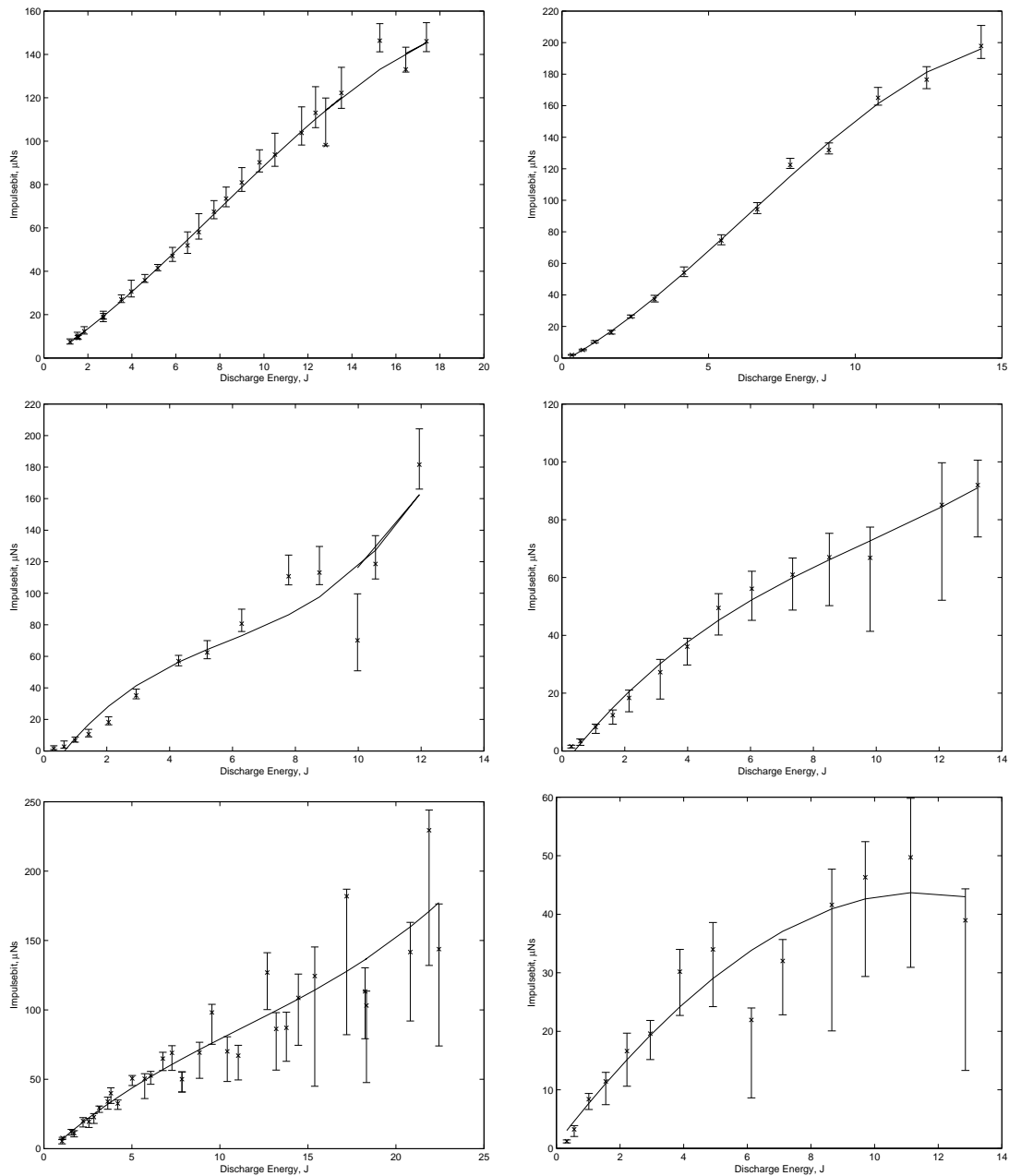


**Figure 2. Top Left: Electrode Separation = 10mm, Top Right: Electrode Separation = 30mm, Middle Left: Electrode Separation = 50mm, Middle Right: Electrode Separation = 70mm, Bottom Left: Electrode Separation = 80mm, Bottom Right: Electrode Separation = 90mm**

The shape of the electrode was chosen to be a thin and blade like, see Figure 3. This geometry was chosen because the presumption was that the blade edge would promote areas of cathode spot erosion and physically ensure they remained in the same location when multiple emission sites formed.

The bladed electrode concept integrated with the decision not to use Teflon was further expanded upon

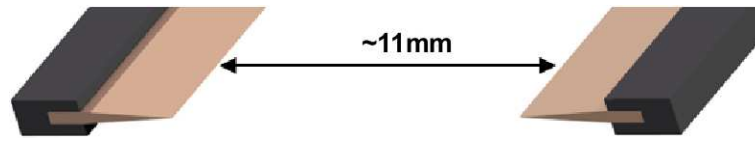


Figure 3. PPT with a new form of electrode design based on a blade geometry

to create a mock up of what a propulsion system may look like, see Figure 4. The propulsion system was initially split into three modules, where 8 PPTs were split into two modules of 4 PPTs per module and a third module was dedicated to a PPU to convert 5V to a high voltage output. The amalgamation of the three modules can be situated within a 2 or 3 unit CubeSat chassis and the placement of the modules within the chassis is flexible to allow for other components and payloads. The design offers control and propulsion in pitch, roll, yaw, X-axis and Y-axis.

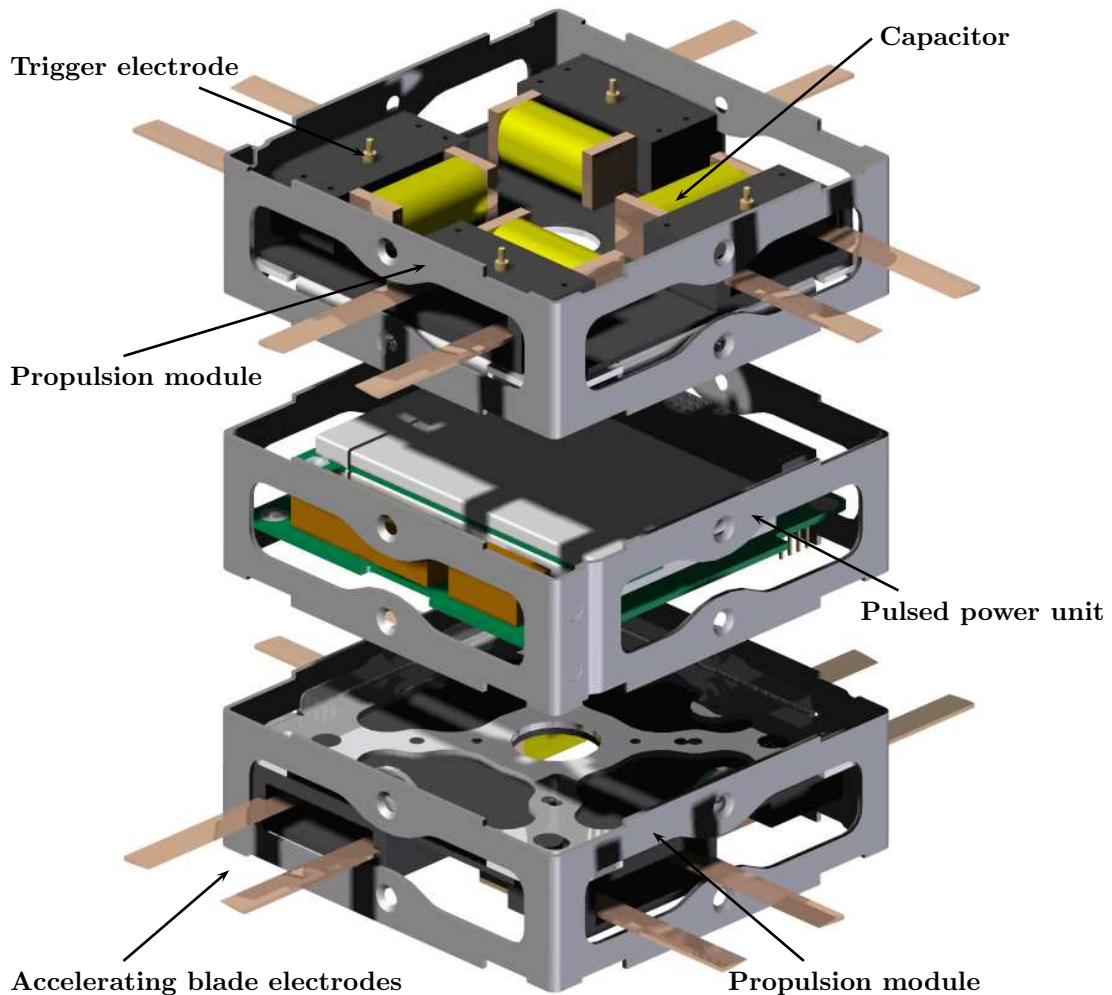


Figure 4. Conceptual design of a CubeSat propulsion system comprised of 3 modules with a total of 8 PPTs to provide X-axis, Y-axis, pitch, roll and yaw motion control in a CubeSat

Initially it was thought that the plane electrodes could be lengthened to provide more material to be eroded and hence increase the overall  $\Delta V$  of the propulsion system. However, CubeSats are designed to be modular and adding protruding electrodes would have meant a redesign of the deployment pod that the CubeSat is launched from, which would have been both costly and complex. Therefore the electrodes were

shortened to remain within the CubeSat chassis. This however decreased the amount of electrode propellant available to the system. To overcome this the electrode width was increased to 0.5mm.

During the design phase careful consideration was taken into developing the discharge initiator. In total there were three concepts that were looked into; the field electron emission effect by the traditional spark plug, thermal electron excitation by semiconductor lasers and a mechanical trigger formed from high voltage contacts breaking. Early on it was shown that laser excitation would be too complex a process to procure, build and control, so it was dismissed. Closer consideration was given to the other concepts. Initially the field electron emission effect was thought to be the ideal choice, as EMCO High Voltage Inc. sold a 5V DC to negative 10kV voltage multiplier in a 1.7cm<sup>3</sup> package. The issue though was total volume. Having one multiplier per thruster sparkplug was an unworkable solution, as space was required for other payloads. To try to overcome this a network of state of the art reed relay switches linked to a single multiplier was investigated. However with each relay being 25 to 30mm long this still took up considerable space.

The high voltage contact breaking method of creating a spark via a mechanical trigger was further developed. The system consisted of a contact arm, a lever arm, a torsion spring, an electromagnet and a retaining pin, see Figure 5. The torsion spring is not shown but should be located around the cylindrical part of the contact arm with one spring leg slotting into the cut out section of the lever arm and the other spring leg attached to the thruster housing (not shown). The lever arm and electromagnet was made from steel and will be used to create a downward force that will pivot the contact arm to make contact with the grounded electrode. Once the electromagnet is turned off the lever arm is restored to its original position by the torsion spring.

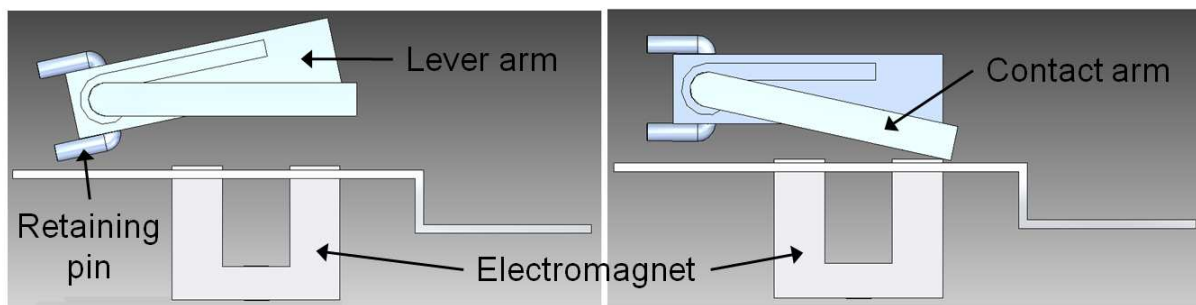


**Figure 5. The high voltage contact breaking trigger system in the up and down positions**

Using the high voltage contact breaking method caused the contact arm to erode and so the separation distance between the electromagnet and lever arm needed to allow for this erosion in its design. The material the contact arm was made from also affected the erosion rate. Using a material with a low erosion rate would extend the lifetime of the contact arm. Although for bread boarding the contact arm would be made from aluminium the actual flight hardware contact arm will be made from Elkonite (75% Tungsten, 25% Copper) due to its low erosion rate but relative ease in manufacture (compared to pure Tungsten), see Figure 6.



**Figure 6. Contact arms. Left: Aluminium, Right: Elkonite**

The capacitor, electrodes and contact arm needed to be isolated from the rest of the spacecraft and its payloads. Ultem<sup>TM</sup> has previous flight experience with flown PPTs and also has a high dielectric strength, so this material was chosen for the thruster housing. The design of the thruster housing, capacitor, electrodes and trigger system can be seen in the cut away diagram shown in Figure 7.

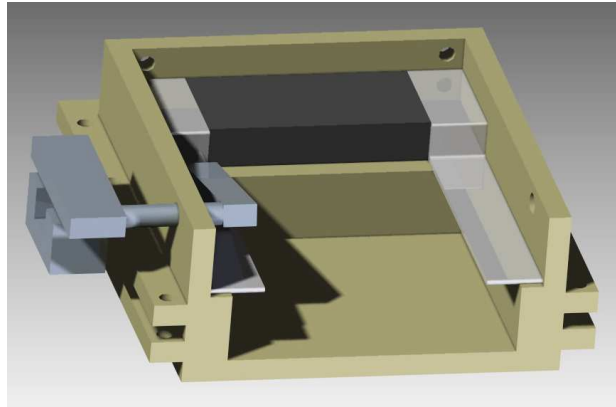


**Figure 7. Mock up of the thruster housing with the electrodes, capacitor and trigger system**

The thruster housing measures  $40\text{mm} \times 40\text{mm} \times 12\text{mm}$  and four of these housings can be situated on a PC104 board in a rotational symmetric off axis configuration see Figure 8. The PC104 requirements are a set of standards that the CubeSat industry uses to provide and allow for modularity. The PC104 system requirements specifically relating to board dimensions were adhered to, to ensure smooth integration with other payloads. However, there was a design conflict with the structural supports and the thruster housings, so additional PC104 boards were placed above and below the thruster module to ensure integration with other payloads but to allow the structural supports within the thruster module to be relocated.

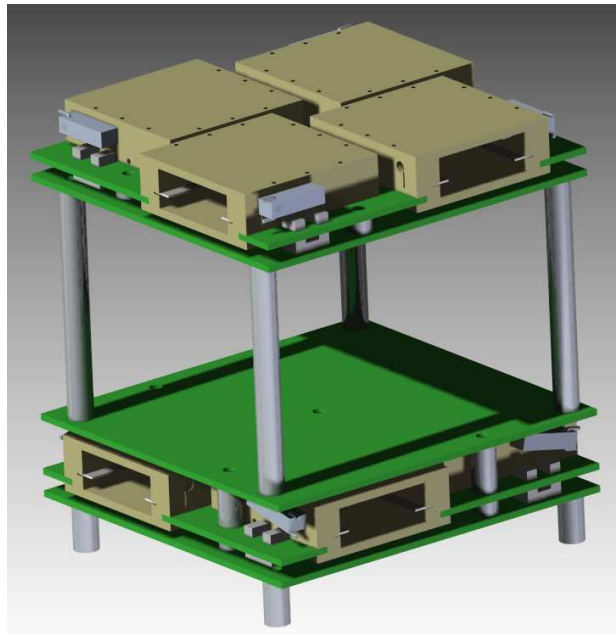


**Figure 8. Mockup of the propulsion module showing the location of all eight  $\mu$ PPT units**

The PPU was designed to charge up the high voltage capacitors within the eight PPTs. The target was set to charge two  $4\mu\text{F}$  capacitors within one second allowing the satellite to fire two thrusters at any one time at a discharge rate of  $1\text{Hz}$ . The capacitors were designed to be charged to  $700\text{V}$  by using a DC to HV DC multiplier. The multipliers were supplied by EMCO High Voltage Inc. and were packaged into a  $12.7\text{mm}^3$  cube. Four multipliers were put into the PPU design. On their input lines  $1\text{kV}$  rated diodes were added to provide reverse polarity protection and  $10\mu\text{F}$  capacitors were added to reduce reflected ripple currents on the input supply lines. The PPT capacitors needed to be isolated from each other so when one triggered it would not cause a cascade effect and discharge all the others. To do this low pass filters made



from 33nF capacitors and 10kΩ resistors were made. The low pass filters were placed before the 4μF high voltage capacitors. Figure 9 shows the built PPU and PPT module after the design phase but before they were tested in the breadboard phase.

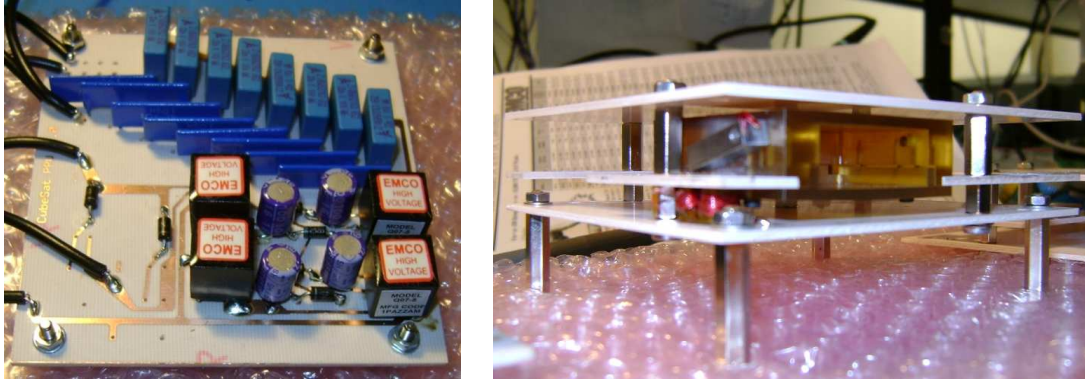


Figure 9. Left: STRaND-1 PPU before bread boarding. Right: STRaND-1 PPT before bread boarding

### III. μPPT Breadboarding Phase

The PPT and PPU were modified after bread boarding the initial design. Several flaws were found in the original design. The design was based on a 4μF capacitor rated at 700V, however the volume available for the capacitors was 3cm<sup>3</sup>. It was a challenge to find a pulse capacitor that would be rated to high voltages and fit into the available volume. The custom capacitor manufacturer Calramic (USA) were able to manufacture two CR09 capacitors fixed by copper tabs in parallel to provide a total capacitance of 0.76μF at 700V, rated for more than 1 million pulses, see Figure 10.

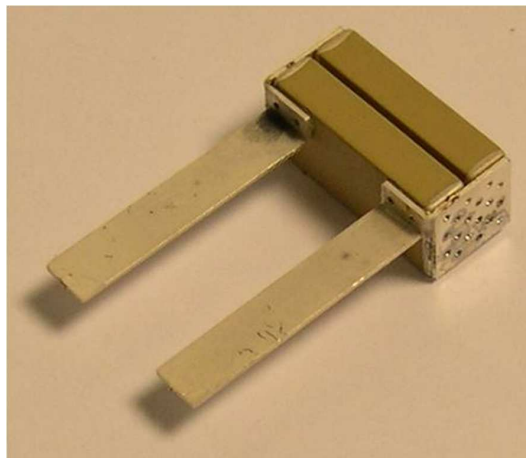


Figure 10. Calramic CR09 pulse capacitor for the STRaND-1 PPT

The electrodes were soldered directly onto the PPT capacitor to reduce circuit inductance and resistance between the two elements. The electrode geometry was 25mm in length, 5mm in thickness, 0.5mm in width and separated from each other by 11mm.

The low pass filter designed to isolate the discharging capacitors from each other had a cut-off frequency of 482Hz. The PPT has a discharge frequency between 30-200kHz. In theory the filter was expected to work however it did not operate satisfactorily. Often when one of the capacitors was discharged or one of the triggers operated, all of the capacitors in the system discharged. This was initially negated by using a 20M resistor instead of the 10KΩ resistor which reduced the cut off frequency to 4Hz. However, this increased the capacitor charge time to around 60 seconds and so was unworkable. The solution was to use a high voltage diode instead of a low pass filter which did not limit the current flow to the capacitor but did stop

the transient effects that caused the other capacitors to discharge.

The charge time of the capacitors was an issue. Using four EMCO DC to HV DC multipliers and bread boarding the initial PPU with a  $2.2\mu\text{F}$  ceramic capacitor (also from Calramic) showed the charge time was around six seconds. Although the CR09 capacitor was only  $0.76\mu\text{F}$ , it was an indication that the PPU would struggle to charge two capacitors in one second. To rectify this, the number of DC to HV DC convertors was increased from four to eight, see Figure 11. This was achievable due to the space saved from the removal of the low pass filters.

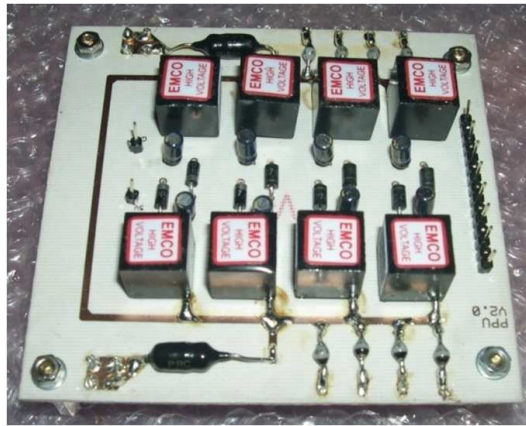


Figure 11. Revised PPU developed during bread boarding for the STRaND-1 CubeSat

The working principle of creating a spark by a lever contact mechanism proved to be a viable option during bread boarding but the design of the original trigger mechanism proved to be troublesome. The original concept used a steel lever arm and electromagnet to provide a downward force and a torsion spring to provide a returning force. However, when assembled there were several problems with this design. When compressed, the torsion spring would press on the pivoting arm creating additional frictional forces. The magnetic field produced by the electromagnet within the set power budget was too weak to overcome the torsion spring stiffness. Finally magnetic remanence within the steel caused it to become permanently magnetised, which would interfere with other systems on the CubeSat.

The electromagnet and lever arm assembly was replaced with a P653 piezo electric motor, see Figure 12. The  $\mu$ motor from Physik Instrumte (PI) GmbH & Co had a 0.15N push-pull capability with a movement range of 2mm and a power consumption of 0.5W. Compared to the electromagnet and lever arm assembly the  $\mu$ motor increased the timing accuracy in which discharges could be triggered.

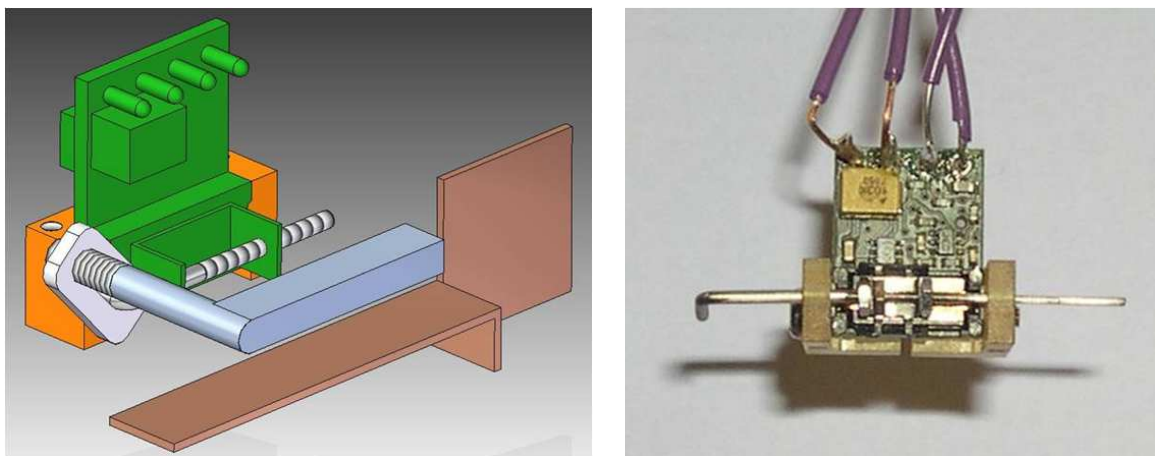


Figure 12. The redesign of the trigger system using a P653 piezo electric motor

Once the system had been built it was found to be extremely delicate. The holder in which the push rod was mounted was susceptible to becoming stuck. In the harsh vibrational environment of a launch, this



was an overwhelming risk. Also the holder in general was not stable and so the rod would rub against the guiding holes in the motor mount which caused frictional forces that the motor was not able to overcome. These issues meant that this avenue of development was dropped and other solutions were investigated.

The next candidate was a simple system using Nitinol wire and a returning force spring. Nitinol wire is a shape memory alloy which has the useful property of contracting when heated. The total contraction is around 10% of the wires total length. Contraction occurs when the crystalline structure in the wire shortens when heat is applied. The wire has a naturally high resistance compared to nominal metal wires and when a current is passed through the Nitinol wire its own resistance became the source of heat. The Nitinol wire activates and contracts between 70-75°C depending on the specific composition of the wire. Convection was the main method of cooling the wire down once it had contracted. During the cooling down phase a returning force spring would return the wire to its original length. The movement created was enough to move the contact trigger arm. A system was designed for the  $\mu$ PPT, see Figure 13, which operated nominally in the laboratory environment.

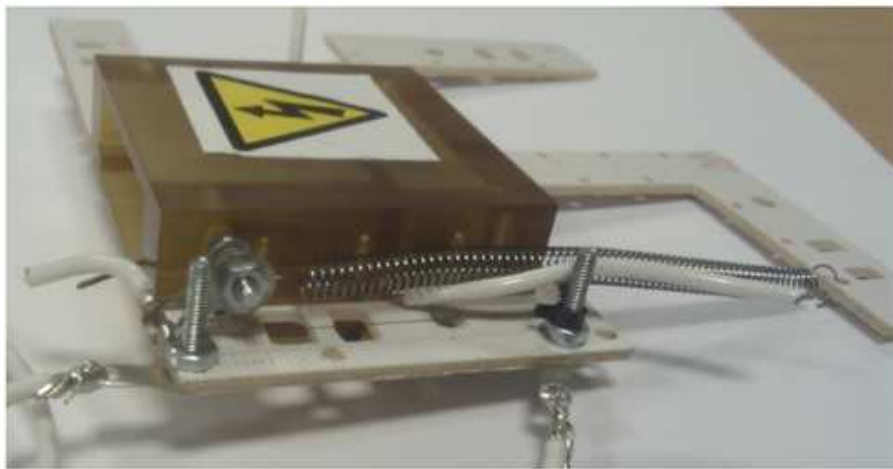


**Figure 13. The redesign of the trigger system using a Nitinol wire and spring mechanism**

Once placed in the vacuum environment, due to the change in the thermal properties of the system, a reduced current was required to contract the wire. However, the main method in cooling was now conduction through the Nitinol wire structural supports and this took around 20 seconds before the trigger mechanism could be operated again. The Nitinol wire was relatively thin and brittle and broke on several occasions whilst under high stress conditions, which, coupled with the slow repetition rate of this mechanism, called into question the survivability of this system during launch.

The last system developed returned to the method of using a piezo electric motor. The SQUIGGLE linear micro motor is manufactured by Newscale Technologies. It uses a system of four pads made from piezoelectric material located around a central threaded rod. The pads are oscillated in such a manner to resemble a 'hula' motion that causes the central threaded rod to rotate around its central axis, which can cause it to move to the extent of the rod length (in this case up to 6mm). The motor has nanometre resolution, provides a force up to 5N and can change the translation speed of the rod from 1-10mms<sup>-1</sup>. The design of this system is shown in Figure 14. Once built the trigger system was tested by being operated 10,000 times, during this test the system operated flawlessly.

An additional problem with all the trigger mechanisms was the possibility that spot welding would occur. The trigger contact arm is charged up to 700V and when brought into contact with the ground electrode caused a spark to occur that would melt the surface of the electrodes, which can cause them to bond or weld together. Limiting the current through the contact arm assembly can reduce the chance of spot welding. Initially a COTS 9Ω resistor was used but after a few tests this resistor blew. The COTS resistor was replaced with a miniature 9Ω resistor rated to 5W and 1kV from the Precision Resistor Company. The new resistor worked well in parallel with the motor which provided enough force to overcome any spot welding that occurred.

Due to some power lines being up to 700V the standard PC104 headers in the CubeSat standard were not implemented into the design. The additional space was used to either accomodate a thruster unit on

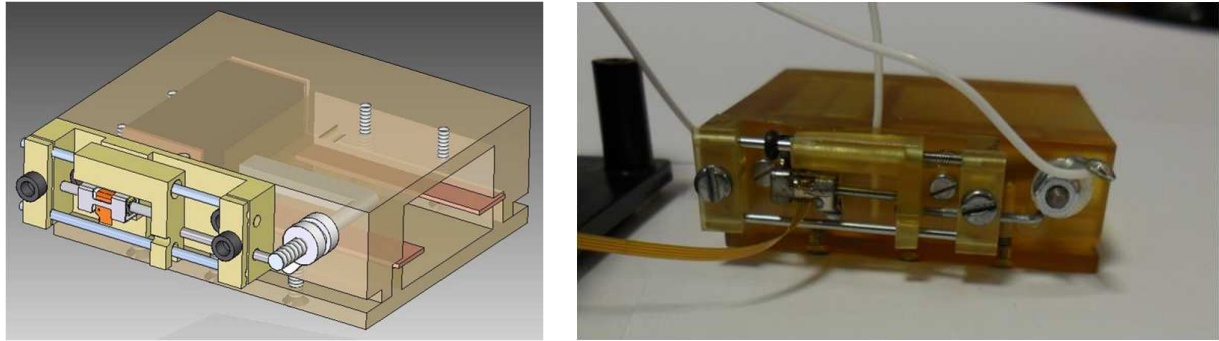


Figure 14. The redesign of the trigger system using a SQUIGGLE motor

the propulsion module boards or make space for clearances around HV lines located on the PPU board. A harness manufactured by Axon cables was constructed and integrated into the design. The connecting wires were made to ESCC 3901.013.01 standards, with connectors made to MIL-M-24519 standards out of a liquid crystal polymer. The harness was rated to 1kV, but when tested in the Surrey Space Centre's large vacuum chamber no breakdown occurred up to the maximum test of 2.5kV.

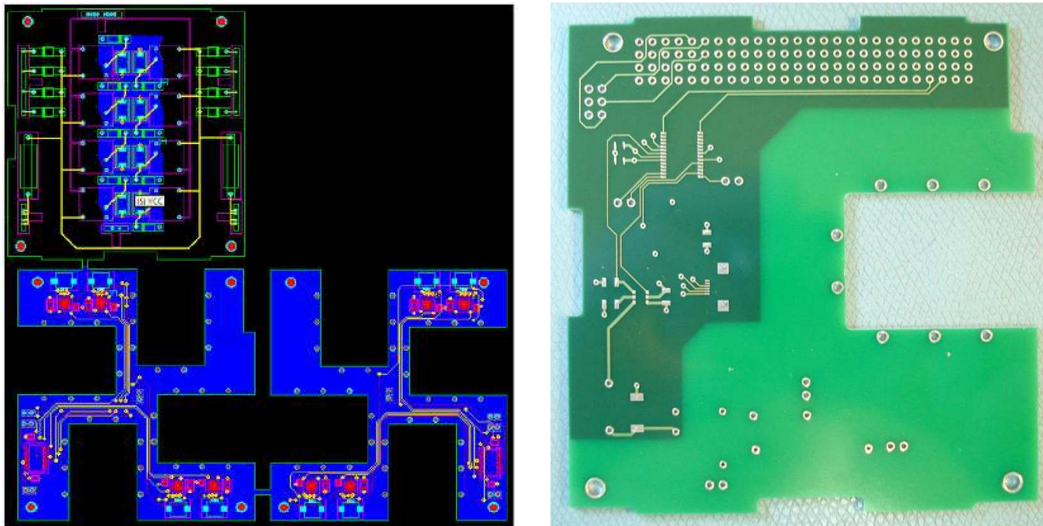


Figure 15. The PCB layout for the STRaND  $\mu$ PPT flight module and the manufactured PCB for the qualification model

The low voltage electronics were then developed. A Texas Instruments power distribution switch was used to limit the current into the PPU to prevent the PPT capacitors drawing too much load too fast from the main satellite battery. Another issue was controlling the SQUIGGLE motors. The motors came with their own NSD 2101 drivers with their own I<sup>2</sup>C commands, which were incompatible with the satellite I<sup>2</sup>C commands. A  $\mu$ -controller was added as a buffer to interpret I<sup>2</sup>C commands from the satellite and translate these into I<sup>2</sup>C commands which the NSD 2101 driver could handle. Once the electronics had been selected they were placed into a PCB layout ready for manufacture. The PCB was a four layer FR4 PCB with a lead Hot Air Solder Level (HASL) finish for ease of component integration.

It was around this time that a second flight opportunity arose to fly a single  $\mu$ PPT on the 3U CubeSat UKUBE-1 mission. The UKUBE-1 mission is the maiden CubeSat mission for the UK Space Agency and although unsuccessful chosen the PPT was downselected to the final six payloads. During this time the UKUBE-1 PPT was developed. After the down selection process it was decided to continue with the manufacture off the PPT board and use it as a qualification module for the STRaND PPT program. Figure 15 shows the PCB layout for the flight module and the manufactured PCB for the qualification model.

Once the  $\mu$ PPT units had been built preliminary testing was conducted in the laboratory environment.

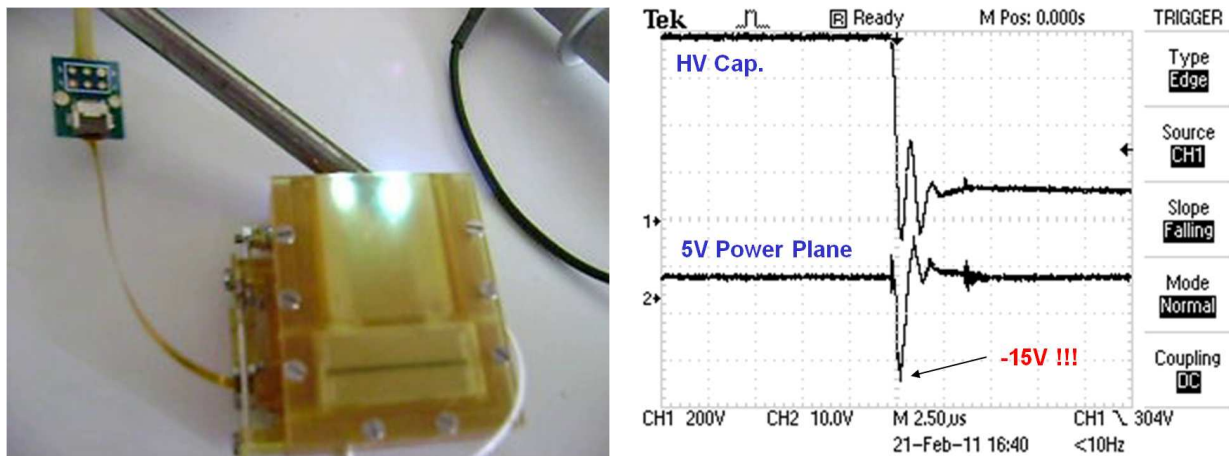


Figure 16. Left:  $\mu$ PPT being discharged in a laboratory environment. Right: Voltage profile across terminal of electrodes and across the power plane

Concerns were raised about possible electromagnetic interference from the pulsing PPTs with the sensitive electronics of the other subsystems. Figure 16 shows the voltage profile of the discharging capacitor and the low electronics power plane. It is noted that in a vacuum environment the frequency of the discharge is less than the one shown. It can be seen that when the PPT fires, a negative 15V spike is seen in the power plane. This would in effect cause all the electronics in the satellite seeing this signal to 'reset'. Obviously this was undesirable and a solution to the issue was sought. The previously introduced current limiting switch only limited the spike to a negative 0.2V on the 5V line with an overall drop in voltage of 5.2V. A second solution was to incorporate a low pass filter. However, this only reduced the magnitude of the ripple rather than eliminating it. The ripple was reduced to approximately 2V. With limited space for filter electronics it was difficult to have a multistage or large low pass filter. The next solution was to try a 5<sup>th</sup> order Butterworth low pass filter, which was a single chip device. The Butterworth filter worked well. However, it was designed for filtering signal lines rather than power lines and so the outputted filtered line was significantly current limited. As this fed directly into the DC to HV DC multiplier this meant the peak voltage seen by the PPT capacitor was only 200V. This rendered this solution unworkable. The final solution came from using a Murata NFM31 single chip power filter with a footprint of 3.2mm  $\times$  1.6mm. The filter was placed both on the 5V line and the ground line to the DC to HV DC multipliers. The filters provided adequate protection and damping of the discharge ripples to less than 100mV on the power planes. However, to incorporate the filters into the flight design two of the DC to HV DC multipliers had to be removed.

Another secondary effect of the discharging PPT was the effect by induction on nearby electronic systems. Figure 17 shows the effect of this induction on a dipole antenna as a function of distance. The  $\mu$ PPT is discharged in a laboratory environment during these tests. The secondary high burst frequency discharges seen should be ignored as these are due to resonance effects between high and low voltage oscilloscope probes which were inputted to the same oscilloscope. The plots show that even at the maximum distance of 30cm, equivalent to the length of the STRaND-1 satellite, an induced ripple of approximately two hundred millivolts was produced and at close distance was over 1.5V. This induced ripple can cause electronic components to reset within the whole of the satellite.

To overcome this a Faraday's cage was placed around the laboratory  $\mu$ PPT which provided adequate protection, see Figure 17. For the qualification model an aluminium Faraday's cage was designed but in practice due to size and volume constraints copper tape with conductive adhesive was affixed around the Ultem housing and grounded, see Figure 18. Additionally ground planes between the PPT modules and the other CubeSat subsystems were added to the internal structure of the CubeSat.

After the bread boarding phase was completed the qualification model and the flight model were built in a clean room environment, see Figure 19. The flight model is partially built, still requiring a Faraday's cage to be applied to each thruster and the trigger mechanisms to be attached.

To accurately measure the current waveform in the discharging PPT requires a rogowski coil, but due to the size and close integration of the electrodes to the capacitor, placing a rogowski coil would directly interfere



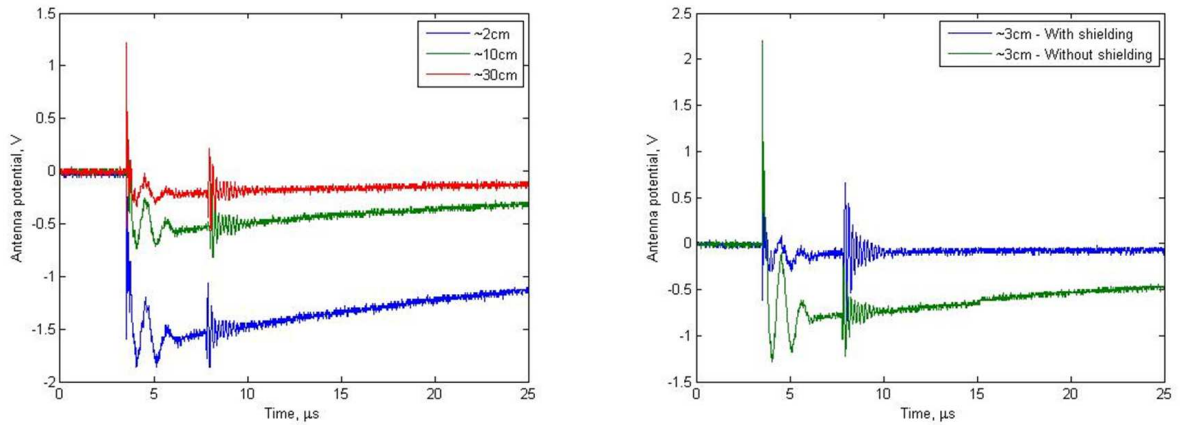


Figure 17. Left: Induced voltage in a dipole antenna as a function of distance. Right: Shielded and unshielded signals

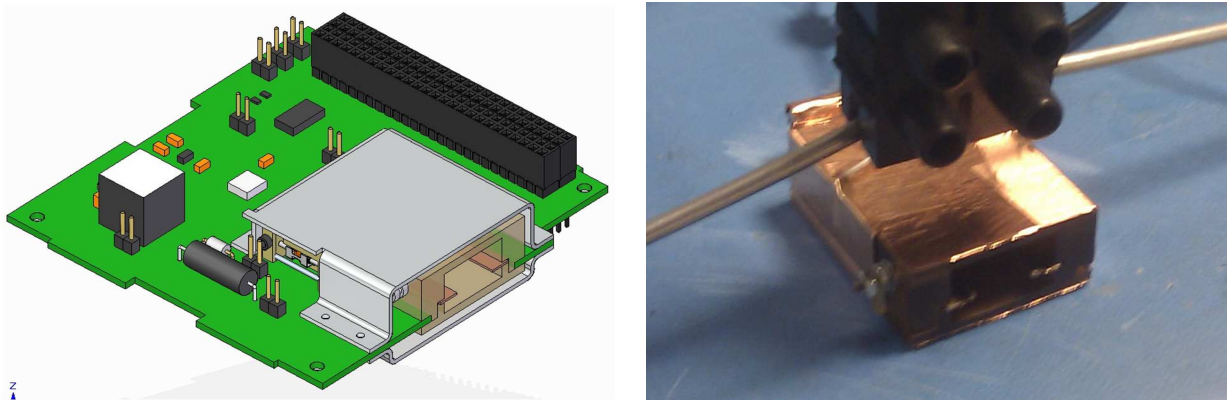


Figure 18. Left: CAD design of the Faraday's cage for the qualification model. Right: Actual Faraday's cage implemented into flight hardware

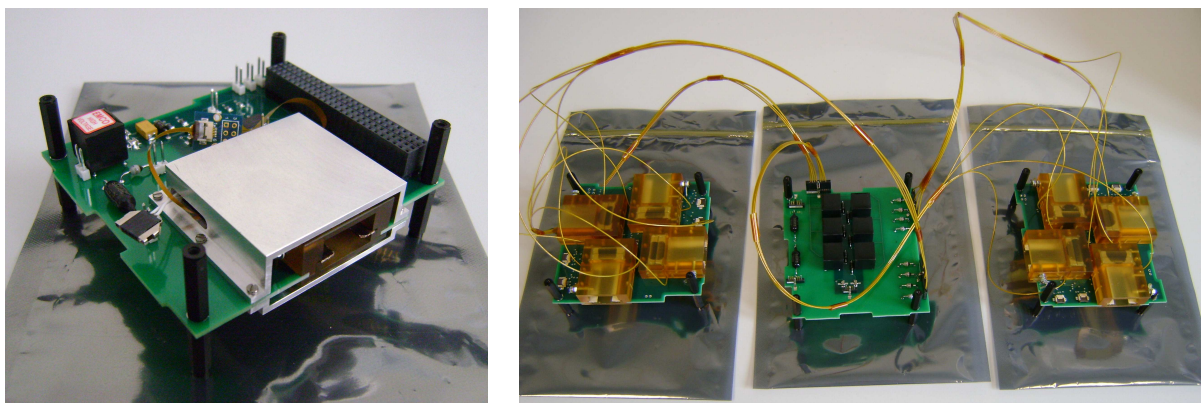
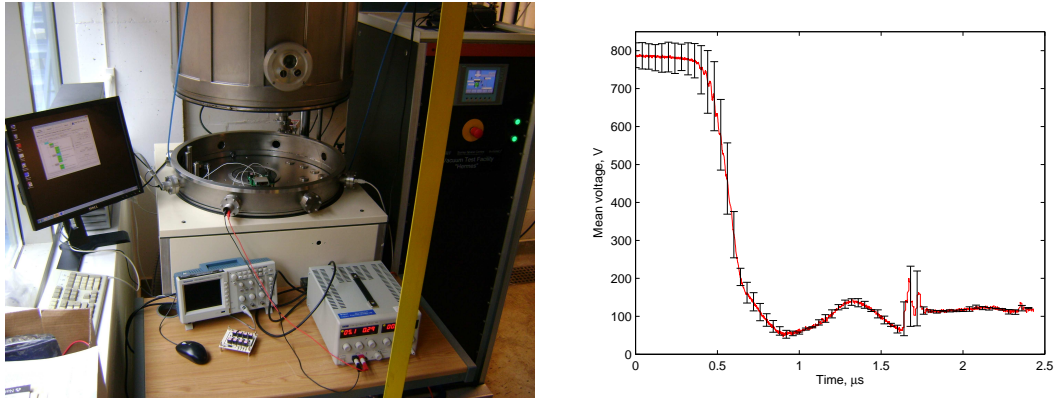


Figure 19. Left: Qualification and lifetime testing module. Right: STRaND-1 PPT flight module

with the dynamics of the discharge gap. A high voltage probe across the capacitor terminals however can give the frequency of the discharge in the vacuum environment. Figure 20 shows the qualification module in the Surrey Space Centre's small vacuum chamber and the typical discharge voltage profile of the  $\mu$ PPT. The voltage profile infers, due to its form, that there is a single strong pulse followed by two or three weaker

pulses. Interestingly after the third pulse a secondary sharp peak occurs between  $1.65\mu\text{s}$  to  $1.75\mu\text{s}$ . The location of this peak is not consistent in time due to the averaging of the data the spike appears to be 100V. However, when investigating the original data the spike was between 260V to 355V. This phenomenon may be caused by the PPT capacitor because it is made from two parallel joined chip capacitors, but further work is required to establish this. It can be estimated from the voltage profile that the frequency of the discharge is 1.25MHz.



**Figure 20. Left: Qualification model in the vacuum chamber discharging. Right: Voltage discharge profile across the capacitor terminals**

Using the frequency the predicted capacitor inductance and resistance can be extrapolated. The resistance of the CR09 capacitor was estimated using an LCR meter and extrapolation to be  $4.1\text{m}\Omega$  and the inductance to be  $18\text{nH}$  at  $1.25\text{MHz}$ . Using the experimental results from the built modules and implementing these into the SSC PPT model,<sup>3</sup> the predicted performance of the STRaND-1  $\mu\text{PPT}$  flight unit is found, see Table 1.

**Table 1. SSC  $\mu\text{PPT}$  target performance based on the results from the developed model**

Parameter	SSC $\mu\text{PPT}$ predicted performance
Propulsion module mass, kg	0.336
Number of $\mu\text{thruster}$ modules	8
Power available to $\mu\text{thruster}$ modules, W	1.5
Bus voltage, V	5.0
Volume required by full $\mu\text{thruster}$ assembly, $\text{cm}^3$	480
Thrust per PPT, $\mu\text{N}$	0.09
Impulse bit, $\mu\text{Ns}$	0.56
Specific impulse, s	321.8
Mass bit, $\mu\text{g}$	0.17

The accuracy of these results needs to be confirmed through flight based experiments. Impulse balances have been developed with resolutions of up to  $1\text{-}10\mu\text{Ns}$ .<sup>2</sup> However, from these preliminary estimated results the impulse bit from the modelled  $\mu\text{PPT}$  would be under its observable limit. A second issue in ground based tests would be the disturbance caused by the movement of the contact trigger arm and the SQUIGGLE motor. It is thought that this disturbance alone will cause enough noise to invalidate any ground based thrust measurements. However, in the space environment the momentum gained by accelerating and expelling material from the thruster should be detectable in the low gravitational environment with long duration tests. It is therefore important to gain flight heritage with these  $\mu\text{PPT}$ s to properly characterise their performance.

In the current configuration the combined PPTs have a total propellant mass of  $1.12\text{g}$ , which equate to a total  $\Delta V$  for the 8  $\mu\text{PPT}$  module for a 3U CubeSat with a mass of  $4.5\text{kg}$  to be  $2.72\text{ms}^{-1}$ . However with the insertion of copper blocks into the established discharge chamber of the current design the total propellant

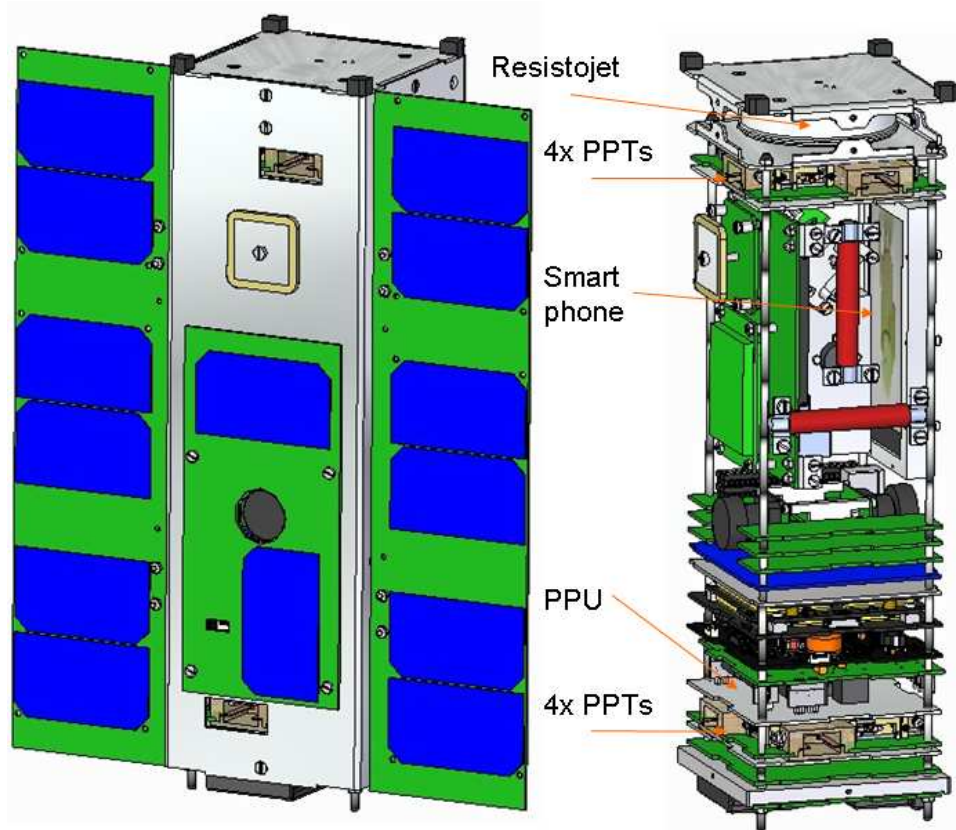


Figure 21. Internal and external views of the STRaND-1 subsystems showing the locations of the resistojet thruster and PPT modules

mass could be increased to 31.3g, which equates to a total  $\Delta V$  of  $76.34\text{ms}^{-1}$ .

The STRaND-1 satellite is currently in the build phase. Since inception the satellite has been used as a tool to train young engineers, both at SSC and SSTL, and has been used to challenge existing manufacturing procedures to understand where costs can be saved in developing future satellites. The CAD model of the STRaND-1 satellite of the complete CubeSat and its internal subsystems can be seen in Figure 21

#### IV. Summary

Based on experimental observations an electric propulsion module with eight  $\mu\text{PPT}$ s has been designed for a 3U CubeSat. During bread boarding the design was evaluated and altered as necessary. The  $\mu\text{PPT}$  module has been specifically designed to meet the PC104 and CubeSat requirements. The  $\mu\text{PPT}$ s have two unique design features not seen in other PPT flown hardware. The first is a contact trigger mechanism that is used to initiate the discharge which replaces the usual sparkplug. The second is the removal of the standard Teflon<sup>TM</sup> propellant which has aided in the miniaturisation of the thruster and allows for four thrusters to be compacted on to a single PC104 board.

Two propulsion modules were developed for two 3U CubeSats: one was for STRaND-1 and the second was for UKUBE-1. STRaND-1 is a joint project between the Surrey Space Centre and Surrey Satellite Technology Limited and was a technology demonstration mission. UKUBE-1 was also a technology demonstration mission run by the UK Space agency. After the unsuccessful down selection of the UKUBE-1 PPT, the module development was continued as a qualification module for the STRaND-1 mission. This was because both  $\mu\text{PPT}$ s used in the modules had an identical design. The qualification and flight units have been built for further testing.

The propulsion module was designed for a 3U CubeSat. Initial results predict that a  $\mu\text{PPT}$  with a specific impulse of 321s, an impulse bit of  $0.56\mu\text{Ns}$  and a mass bit of  $0.17\mu\text{g}$  has been developed. Although



the current design only provides a predicted  $\Delta V$  of  $2.72\text{ms}^{-1}$ , with a relatively simple modification this can be increased to  $76.34\text{ms}^{-1}$ . This would be able to compensate for drag, gravity gradient perturbations and maintain pointing to a high degree of accuracy. Depending on the initial orbit insertion the propulsion module may also provide the ability for the CubeSat to meet its deorbit requirements.

If the launch is successful, STRaND-1 will break two propulsion records: it will be the first CubeSat to have full 3-axis propulsive capabilities and it will be the first time electric propulsion has been used on the CubeSat class of satellite platform. If STRaND-1 is successful this will be a great achievement and will highlight the advantages of using the Pulsed Plasma Thruster on small satellites.

## References

- <sup>1</sup>Shaw, P. and Lappas, V., "Modeling of a Pulsed Plasma Thruster; Simple Design, Complex Matter," 3/6/2010 2010.  
<sup>2</sup>Krejci, D., Seifert, B., and Scharlemann, C. A., "Thrust measurement of a micro pulsed plasma thruster for CubeSats," 24-29 January 2011 2011.  
<sup>3</sup>Shaw, P. V. and Lappas, V. J., "A high current cathode plasma jet flow model for the Pulsed Plasma Thruster," September 1115, 2011 2011.